Direct visualization at the single-cell level of siRNA electrotransfer into cancer cells

Aurélie Paganin-Gioanni, Elisabeth Bellard, Jean-Michel Escoffre, Marie-Pierre Rols, Teissié Justin, Muriel Golzio

Direct visualization at the single-cell level of siRNA electrotransfer into cancer cells

A. Paganin-Gioanni[a,b], E. Bellard[a,b], J. M. Escoffre[a,b], M. P. Rols[a,b], J. Teissié[a,b,1], and M. Golzio[a,b,1]

[a]CNRS (Centre National de la Recherche Scientifique), IPBS (Institut de Pharmacologie et de Biologie Structurale), 205 route de Narbonne, F-31077 Toulouse, France; and [b]Université de Toulouse, UPS (Université Paul Sabatier), IPBS (Institut de Pharmacologie et de Biologie Structurale), F-31077 Toulouse, France

Edited by Richard Heller, Old Dominion University, Norfolk, VA, and accepted by the Editorial Board May 16, 2011 (received for review March 3, 2011)

The RNA interference-mediated gene silencing approach is promising for therapies based on the targeted inhibition of disease-relevant genes. Electropermeabilization is one of the nonviral methods successfully used to transfer siRNA into living cells in vitro and in vivo. Although this approach is effective in the field of gene silencing by RNA interference, very little is known about the basic processes supporting siRNA transfer. In this study, we investigated, by direct visualization at the single-cell level, the delivery of Alexa Fluor 546-labeled siRNA into murine melanoma cells stably expressing the enhanced green fluorescent protein (EGFP) as a target gene. The electrotransfer of siRNA was quantified by time lapse fluorescence microscopy and was correlated with the silencing of *egfp* expression. A direct transfer into the cell cytoplasm of the negatively charged siRNA was observed across the plasma membrane exclusively on the side facing the cathode. When added after electropulsation, the siRNA was inefficient for gene silencing because it did not penetrate the cells. Therefore, we report that an electric field acts on both the permeabilization of the cell plasma membrane and on the electrophoretic drag of the negatively charged siRNA molecules from the bulk phase into the cytoplasm. The transfer kinetics of siRNA are compatible with the creation of nanopores, which are described with the technique of synthetic nanopores. The mechanism involved was clearly specific for the physico-chemical properties of the electrotransferred molecule and was different from that observed with small molecules or plasmid DNA.

electroporation | transfection | gene therapy | imaging | targeting

Since its discovery by Fire et al. in 1998, RNA interference represents a promising approach towards the inhibition of gene expression not only in cell culture but also in vivo for the development of new generation biodrugs (1). Small interfering RNA (siRNA) is not only used for basic scientific research; the efficiency of siRNA therapeutics against a variety of diseases is now being evaluated in preclinical and clinical trials (2–5). There is a common opinion that the full potential of siRNA as a therapeutic agent will not be attained until better methodologies for its targeted intracellular delivery to cells and tissues are developed (4, 6, 7). Highly negatively charged oligonucleotides, such as naked siRNA, can barely cross the cell membrane to reach the cytoplasm where their target and their enzymatic machinery are present (5, 8, 9).

Electric pulses are known to strongly stimulate the cell uptake of various molecules showing intrinsically very poor transmembrane crossing abilities (10, 11). The exact mechanism leading to enhanced intracellular nucleic acid delivery remains unclear but it may involve, at least in vitro for plasmid DNA (pDNA), the induction of local physical interactions between the nucleic acid and the cell membrane followed by a slow intracellular release into the cytoplasm (12, 13). In vivo, electric pulses have been extensively used for drugs, siRNA, and pDNA delivery into a large number of organs and tissues (14–17). In rodents, electric pulses have been used to deliver siRNAs into various organs (15, 18–20). siRNA delivery led to an efficient gene silencing when transferred into a tumor where their biodistribution was found to be homogeneous throughout the cytoplasm of electropermeabilized cells (21). In addition, the delivery of molecules is restricted to the volume where the electric field (EF) is applied. Only a very few short-lived side effects have been reported for these treatments, emphasizing the innocuity of this physical method for clinical use (22). Indeed, electrochemotherapy, the electrotransfer of cytotoxic drugs into tumors, is a routine clinical methodology in Europe, and electrogenotherapy, the electrotransfer of therapeutic genes into tissues, is undergoing preclinical trials [e.g., ESOPE (European Standard Operating Procedures of Electrochemoterapy) and Angioskin European projects, Inovio Biomedical Corp. (23, 24)]. Moreover, siRNAs delivered directly into the cytoplasm by electropulsation do not induce inflammatory responses, as reported with other delivery approaches (22). Although electropermeabilization (EP) shows promise in the field of new therapies, very little is known about the molecular processes supporting RNA transfer across the plasma membrane to the cytoplasm where it reaches the RNA-induced silencing complex (RISC).

On a B16F10 mouse melanoma cell line stably expressing the enhanced green fluorescent protein (EGFP), we first evaluated the dose dependence and the impact of labeling siRNA upon *egfp* expression level after its electrotransfer into cells. In order to assess the relative contribution of the EF and to investigate the processes that support siRNA electrotransfer in melanoma cells, we studied the localization of fluorescently labeled siRNA at the single-cell level by using time lapse fluorescence confocal microscopy. This strategy was performed in our previous study of pDNA electrotransfer (13). We observed that the electrophoretic drag allows a direct access of siRNA into the cytoplasm where its enzymatic machinery and target are present. The transfer kinetics of siRNA are compatible with the observations on synthetic nanopores, but they differ from other molecular electrotransfers, such as the electrotransfer of small molecules (e.g., propidium iodide) or pDNA.

Results

Effect of the *egfp* siRNA Electrotransfer In Vitro. In order to determine the efficiency of siRNA electrotransfer, we used *egfp* siRNA molecules targeting the mRNA of the EGFP constitutively expressed in B16F10-EGFP melanoma cells (14). Optimal electrical parameters for EP and the associated electrotransfer were determined by monitoring both the penetration of propidium iodide (PI) into cells and cell viability. These parameters

Author contributions: J.T. and M.G. designed research; A.P.-G. performed research; E.B., J.M.E., and M.P.R. contributed new reagents/analytic tools; A.P.-G., E.B., J.T., and M.G. analyzed data; and A.P.-G., J.T., and M.G. wrote the paper.

The authors declare no conflict of interest.

This article is a PNAS Direct Submission. R.H. is a guest editor invited by the Editorial Board.

[1]To whom correspondence may be addressed. E-mail: muriel.golzio@ipbs.fr or justin.teissie@ipbs.fr.

This article contains supporting information online at www.pnas.org/lookup/suppl/doi:10.1073/pnas.1103519108/-/DCSupplemental.

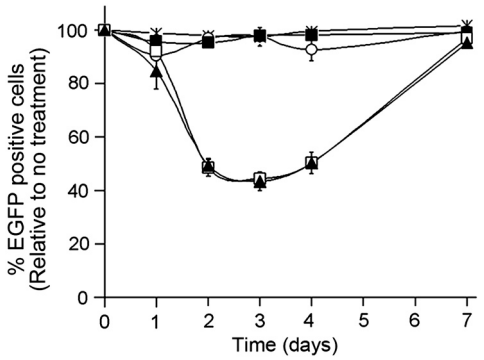

Fig. 1. Effectiveness of siRNA silencing after electrotransfer in vitro. The relative percentages of cells expressing *egfp* were quantified by flow cytometry as a function of time. The cell suspension was electropermeabilized [(snowflake) EP] (10 pulses of 5 ms, 500 V/cm, 1 Hz) in the presence of 2 μg of unrelated siRNA [(empty circle) unrelated siRNA + EP], 2 μg of *egfp* siRNA [(empty square) *egfp* siRNA + EP)] or 2 μg of *egfp* siRNA labeled with Alexa Fluor 546 [(solid black triangle) AF-546 siRNA + EP]; 2 μg of *egfp* siRNA alone was also tested [(solid black square) *egfp* siRNA]. The error bars represent the SD of three independent experiments.

(10 pulses, 5 ms duration, 500 V/cm at 1 Hz) led to 67.2± 1.4% of permeabilized cells and 73.3 ± 0.8% cell viability [see (21)]. The percentage of permeabilized viable cells was 40.4± 0.8% (25).

The percentage of cells still expressing *egfp* (EGFP-positive cells) was quantified after siRNA electrotransfer by flow cytometry as a function of time (Fig. 1). The expression of *Egfp* was hardly affected in all of the controls. Indeed, if an unrelated siRNA was electrotransferred into B16F10-EGFP cells, the percentage of EGFP-positive cells was not modified. As expected, the electrical treatment itself had no effect. If no EP was applied in the presence of *egfp* siRNA, no *egfp* silencing was observed. In contrast, *egfp* siRNA electrotransfer led to a significant decrease in EGFP-positive cells within 2 d after the treatment. A reduction of 50–57% of *egfp*-expressing cells was observed at days 2, 3, and 4. This reduction was in agreement with the percentage of permeabilized cells in the surviving population (40.4% out of 73.3%, i.e., 55%). These results support the conclusion that siRNA was electrotransferred in all (100%) permeabilized and viable cells.

The lag observed in Fig. 1 for the silencing to reach a maximal level was in agreement with the 24 h half-life reported for EGFP in cells. The effect of siRNA was transient; the percentage of cells expressing *egfp* returned to the initial value at day 7. A dose-dependent effect was observed with a maximum effectiveness with 2.0 μg of siRNA (Fig. S1).

Alexa Fluor 546 (AF-546) labeled *egfp* siRNA electrotransfer (AF-546 siRNA + EP) showed the same silencing efficiency as unlabeled siRNA on *egfp* expression as already reported in Fig. 1 (21). Therefore, it was used in further experiments for the visualization of its transfer within the cytoplasm.

Direct Single-Cell Visualization of siRNA Electrotransfer. In order to investigate the siRNA import into cells, we first analyzed the visualization of the PI entrance both during and after electric pulse delivery by confocal microscopy. The inflow of PI was quantified by the associated fluorescence intensity increase in the cytoplasm (Movie S1). Free diffusion of PI was observed across permeabilized parts of the membrane facing the anode and the cathode, as already published for CHO (Chinese Hamster Ovary) cells (26) and predicted by Tekle et al. (27). Permeabilization was effective (100%), viability was preserved (95%), and the half-time of the permeabilization was 3 min (Fig. S2).

We visualized the first steps of siRNA import into the cells by adding AF-546 siRNA to adherent cells. Before EP, no spontaneous uptake or direct interaction with the plasma membrane was observed (Fig. S3). During pulse application, labeled siRNA penetrated the cell. The penetration took place through the membrane on the side of the cell facing the cathode (Fig. 2*A*, Movie S2). The entrance of the siRNA molecules was detected with the first pulse. At the end of the train of electric pulses, siRNA fluorescence was only observed in the cytoplasm of the cells. No fluorescence was seen in the nucleus (Fig. 2*A*). In Fig. 2*B*, a light profile parallel to the EF direction allowed the quantification of fluorescence intensity (FI) due to siRNA inflow. These results showed the unidirectional entrance of siRNA during the EF application. Statistical analysis of the FI profiles confirmed that this labeling was restricted to the cathode-facing side of the membrane in 98.2 ± 1.3% of the cells, and only 1.8 ± 1.3% of the cells were slightly labeled on both sides. No siRNA electrotransfer occurred on the side of the membrane facing the anode (Fig. 2*C*), whereas the PI experiments showed that this side was permeabilized (Movie S1).

Therefore, siRNA import occurred at the level of the membrane cap facing the negative electrode and directly reached the cell cytoplasm. These data supported the model in which the electrophoretic forces drove the negatively charged siRNA molecules inside the cell.

The Involvement of Electrophoretic Forces in the siRNA Electrotransfer Mechanism. In order to further characterize the mechanism of siRNA electrotransfer and to determine the occurrence of electrophoretic processes in the delivery, we measured the mean fluorescence intensities (MFI) into the cytoplasm before, during, and 1 min after the electric pulse train (Fig. 3). Before EP, the basal fluorescence level in the cells was null. After the first pulse

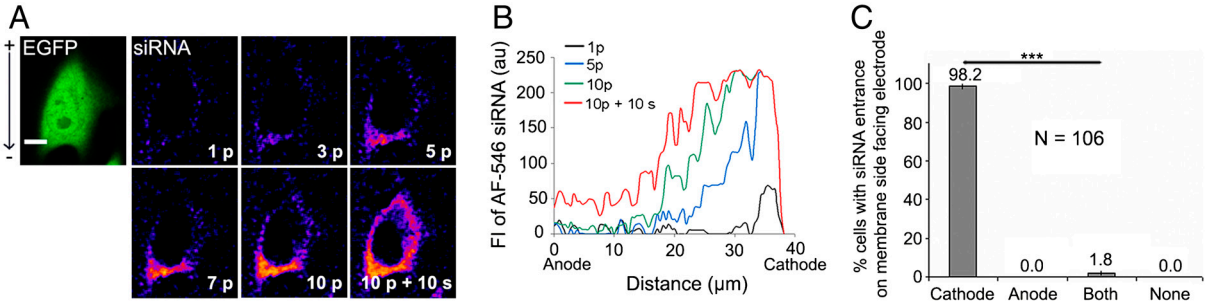

Fig. 2. Direct visualization of the siRNA electrotransfer into cells by confocal fluorescence microscopy. (*A*) AF-546 siRNA was added before applying the EF. The positive electrode was located on the top of each picture. One scan was carried out with the confocal microscope to detect the cells expressing *egfp* (green picture) and a series of scans were carried out to detect AF-546 siRNA entrance during the EF pulse train application (10 pulses, 5 ms, 300 V/cm, 1 Hz) (pseudocolor pictures). An image differential treatment was applied to remove the external fluorescence (see *Experimental Procedures*). (*B*) A representative light plot profile parallel to the EF direction was drawn to quantify the siRNA fluorescence signal across the cytoplasm as a function of time. (*C*) The percentage of cells showing siRNA entrance into the cytoplasm across the plasma membrane facing the cathode, anode, both, or no electrodes was analyzed; $N = 106$.

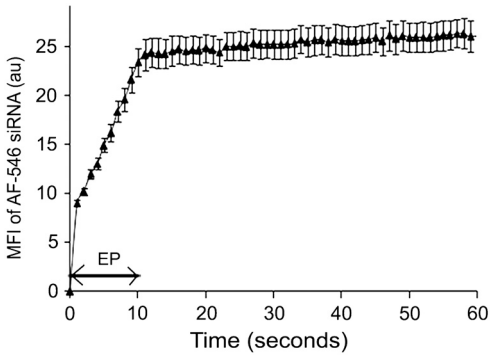

Fig. 3. Quantification of siRNA electrotransfer into cells. The MFI of intracellular AF-546 siRNA was quantified as a function of time during and after pulse application; $N = 38$.

(1 p), the MFI within the cells sharply increased. During the pulse train delivery, a linear increase in the fluorescence was observed. After pulse treatment, no significant increase in the MFI was observed. These observations were in agreement with the electrophoretic migration of the siRNA into the cell but only during the field pulse.

The polarity of the electrodes was then changed between each pulse in order to determine whether or not the electrophoretic forces could push the siRNA molecules alternatively in two opposite directions. Successive scans were acquired during the pulse train and after EP (Fig. 4*A*; Movie S3). The FI always increased on the side of the cell facing the cathode during each pulse, meaning that entry of the siRNA was driven under the control of the polarity of the EF pulse (as expected). The plot profiles after the sixth pulse of the electropermeabilized cells under uni- and bipolar conditions are shown in Fig. 4*B*. The labeled siRNA was detected in the cytoplasm on the side facing the cathode under the unipolar condition, whereas it was observed on both sides facing the electrodes under the bipolar condition.

In order to confirm that a postpulsation diffusion process was not happening, we added siRNA immediately (0 s) or 5 s after EF application (Fig. S4). No decrease in the percentage of EGFP-positive cells was observed 72 h after EP. These results confirmed the theory that siRNA molecules could not enter the cell cytoplasm after EP by a diffusion process as PI did, even if the membrane was still permeabilized, as shown by the PI experiments (Fig. S2).

Discussion

Our results are direct observations of the early events leading to siRNA electrotransfer into tumor cells. In the absence of an EF, no interaction between the siRNA and the plasma membrane was observed, nor was there any penetration into the cells. Under this condition, the siRNA had no effect on *egfp* expression, and no silencing was obtained. In contrast, when the cells were electropermeabilized in the presence of *egfp* siRNA, the percentage of *egfp* expressing cells dramatically decreased 2 d after electrotransfer and returned to the initial value 7 d after the treatment (Fig. 1). The silencing of *egfp* expression was effective and concerned 100% of the permeabilized and viable cells. A delay of 48 h was observed, mainly because of the 24 h lifetime of the EGFP (28). The silencing was transient because we used a synthetic siRNA with no chemical modifications and therefore it could be degraded by intracellular nucleases (29–31). Moreover, the intracellular concentration was decreased by cell division (32).

A few minutes after electrotransfer, the cellular localization of the siRNA was observed spread homogeneously throughout the cytoplasm (Fig. 2; Fig. S5, Movie S2). This homogeneous localization means that the siRNAs had direct access to the enzymatic machinery (RISC) and their target (mRNA). No siRNA was detected in the nucleus of viable cells. This observation suggested that it did not pass through nuclear pores via this transfer method.

The mechanism of siRNA electrotransfer can be compared to the electrotransfer mechanisms of PI and pDNA (Fig. 5; Movie S1; Movie S2; Movie S4) (13). Propidium Iodide fluorescence gave access to the EP events (33). As was already observed during the very first millisecond after or during the pulse (26), the field strength controlled the part of the cell surface where the permeabilized state was detected. Under the present pulsing conditions, in which successive millisecond pulses were applied, the plasma membrane became permeabilized on the two opposite sides facing the electrodes where a free exchange of PI was observed (Movie S1) (13).

In the case of pDNA, these macromolecules interacted with the plasma membrane by forming long-lived localized spots on the electropermeabilized part of the cell membrane. This pDNA/membrane interaction occurred on the side where they were accumulated by the field associated electrophoretic drag (Movie S4). Translocation within the cytoplasm was another step that happened several minutes after the pulse train (13, 34).

In the present study, we observed that electrotransferred siRNA passed through the plasma membrane of cells during electropulsation. The siRNA migrated against the field direction by electrophoresis and penetrated the cytoplasm (Fig. 2; Movie S2). This observation was further supported by quantification of the intracellular siRNA-associated fluorescence as a function of the number of pulses and by the observation that inversion of the EF polarity led to a fluorescent labeling of opposite sides in the cell cytoplasm (Fig. 4; Movie S3).

Electrophoretic movements of the nucleic acids are involved in their transfer into cells. Nevertheless, a different behavior was observed with siRNA. No complex between the siRNA and the cell surface was present during the EF application (no fluorescent

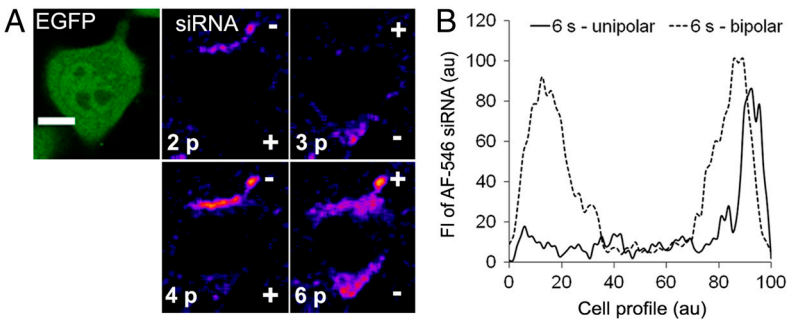

Fig. 4. Direct visualization of the electrophoretic migration during the siRNA electrotransfer under the bipolar condition. AF-546 siRNA was added before applying the EF (8 pulses, 5 ms, 300 V/cm, 1 Hz). (*A*) Representative picture of a cell before the EF. One scan was carried out with the confocal microscope to detect the cells expressing *egfp* (green picture). A series of scans were carried out at a velocity of 1 s per scan with only the excitation of AF-546 siRNA (pseudocolor pictures). (*B*) Representative light plot profiles parallel to the EF direction (at the sixth second) were plotted for unipolar and bipolar conditions.

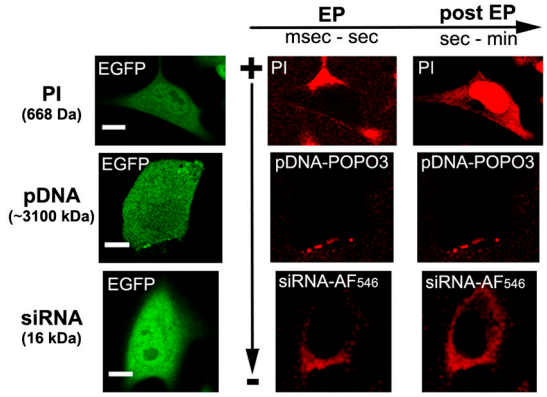

Fig. 5. Electrotransfer of PI, siRNA, and pDNA into murine melanoma cells (10 pulses, 5 ms, 300 V/cm, 1 Hz). The column on the left shows the EGFP-expressing cell. The EP is on the top of the first step of the electrotransfer of PI: penetration can be observed on both sides facing the electrodes during EP. Post-EP (on the right), diffusion and nuclear labeling can be observed. The EP in the center row is the first step of the electrotransfer of pDNA labeled with POPO-3: a localized interaction with the plasma membrane (fluorescent spots) is present on the side facing the cathode and remains present post-EP (on the right) before translocation into the cytoplasm (not detected on this time scale). The EP on the bottom is the first step of the AF-546 siRNA electrotransfer: a rapid and free penetration into the cytoplasm on the side facing the cathode was present during the electric pulses. Post-EP, the AF-546 siRNA was localized diffusely throughout the cytoplasm with no further entry.

spots). The siRNA went through the membrane during the EF application and stopped its penetration after EP. siRNA did not penetrate the cells by the phenomenon of diffusion even though membrane resealing was not completed. This siRNA movement across electropermeabilized cell membranes is relevant to that which occurs with synthetic nanopores.

Indeed, nanopores have emerged as molecular counters and for biomolecule detection with great promise for single-molecule analysis (35–37). A 58 bp dsDNA can be forced through a 2.0 nm diameter pore in a 10 nm membrane only if the voltage applied is $V > 2.75$ V (38). Nanopores (diameter of 3 nm) in synthetic membranes as thin as lipid membranes (5–6 nm) were recently obtained. These pores allow the detection of nucleic acids only 10 bp long as well as the discrimination of differences in their physical dimensions. The conclusion was that 22 bp dsRNA can cross such a biomimetic permeabilized membrane under a 300 mV transvoltage in less than 1 ms (35). This observation gives strong experimental support to our conclusion that siRNA can cross an electropermeabilized membrane in milliseconds under external field-mediated electrophoresis. Under our experimental conditions, the transmembrane voltage across the electropermeabilized membrane was kept at the threshold value (39), known to be about 250 mV (40), and the pulse duration was 5 ms (i.e., much longer than the transit time across the biomimetic membrane).

Altogether, these results show that siRNA molecules have rapid and direct access to the cytosol. Rapid access avoids exo- and endogenous siRNA degradation (22). Direct access to the cytosol is an important advantage along the endocytosis pathway, which is described for chemical methods. The siRNA molecules have to escape from the endosomal compartment, which may increase the immune response via the activation of TLR receptors (41, 42).

Due to the good correlation between the visualization of the siRNA entrance and the resulting gene expression silencing, these results show that the EF-mediated electrotransfer of siRNA in cancer cells is an efficient method of delivery. When the EF is applied, the plasma membrane becomes permeabilized on the sides of the cells facing the electrodes and negatively charged siRNA migrates electrophoretically through the plasma membrane only on the cathode side, resulting in a direct cytosolic localization. After electric treatment no diffusion process takes place, even if the plasma membrane is still permeabilized. This physical method is a powerful tool for siRNA delivery in cancer cells (22, 43). Our conclusions give practical guidance for clinical protocols of siRNA delivery: for efficient delivery, siRNA has to be injected into the target tissue before applying the EF. siRNA only enters cells during pulse application.

Experimental Procedures

Cells. The B16-F10 mouse melanoma cells expressing the EGFP were obtained after retroviral transduction and maintained in culture according to a previously described protocol (14).

Molecules. Propidium Iodide was purchased from Sigma Aldrich. All siRNAs were purchased from Qiagen Xeragon. The *egfp* siRNA duplexes were designed according to Caplen et al. and labeled with Alexa Fluor 546 at the 3′ position of the sense strand (44). The labeling of the siRNA does not significantly modify the global negative charge of the native siRNA. The unrelated siRNA was directed against an unrelated mRNA, and showed no significant homology to the mouse transcripts. The sequences were given in ref. 21. A 4.7 kb plasmid pEGFP-C1 (Clontech) carrying the *egfp* gene was stained stoichiometrically with the DNA intercalating dye POPO-3 (Molecular Probes-Invitrogen), according to the protocol of the manufacturer.

Electrotransfer Apparatus. Electropulsation was operated by using a CNRS cell electropulsator (Jouan), which delivered square-wave electric pulses. An oscilloscope (Enertec) monitored pulse shape. A polarity inverter built in the laboratory allowed the triggering of pulses with alternating (bipolar) polarities. For electrotransfer of siRNAs in cell suspension, the EP chamber was designed using stainless steel parallel plate electrodes (10 mm length, 0.5 mm thick, and 4 mm interelectrode distance), brought into contact on 35 mm Petri dish (Nalge Nunc International). To avoid an electric drift of the cells during pulsation, adherent cells were grown on a glass coverslip chamber for fluorescence microscopy observations (Lab-Tek™ II system, Nalge Nunc International). The EP chamber was designed using two stainless steel parallel rods (1 mm diameter, 10 mm length, 5 mm interelectrode distance) (45). The electrodes were connected to the pulse voltage generator and a uniform electric field was generated. The chamber was placed onto the stage of an inverted confocal microscope (Zeiss LMS510, Carl Zeiss, MicroImaging GmbH) to visualize the siRNA electrotransfer.

Electrotransfer. Cell permeabilization was performed by applying the electrical pulses required to transfer genes and load macromolecules into cells (46). Ten pulses of 5 ms, at a frequency of 1 Hz were applied at 500 V/cm for the cell suspension and at 300 V/cm for the plated cells. On the plated cells, the pulsed EF had to be lowered slightly due to the difference in cell geometry in order to preserve viability. The cells were harvested by trypsinization, washed, and resuspended in the pulsation buffer (10 mM phosphate; 1 mM $MgCl_2$; 250 mM sucrose; pH 7.4). For each assay, 100 μL of the cell suspension was used, corresponding to 10^6 cells. Then, 2 μg of siRNA was added. Five minutes after pulse delivery, the transfected cells were cultured in a 35 mm Petri dish by adding completed culture medium. Over 7 d, the cells were analyzed by flow cytometry after trypsinization (FACScan, Becton Dickinson) to determine the percentage of *egfp*-expressing cells and their associated fluorescence intensity. For fluorescence microscopy observations, 7×10^4 adherent cells on the microscope glass coverslip chamber were treated in 400 μL of pulsation buffer in presence of 100 μM of PI or 4 μg of labeled siRNA or 2 μg of POPO-3-labeled pDNA.

Confocal Fluorescence Microscopy. Confocal microscopy was used to follow the import of PI, labeled siRNA, and labeled pDNA. These molecules were detected using a Zeiss LMS510 inverted confocal laser scanning microscope equipped with a 514 nm Helium-Neon laser. A Zeiss 40× objective (1.3 numerical aperture, oil immersion) was used. Successive scans of less than 1 s were performed to observe the transfer of the siRNA into cells. Cells constitutively expressing *egfp* were observed with a 488 nm Argon laser. Laser power and photomultiplier settings were kept identical for all samples to make the results comparable. Eight bit images were recorded using the Zeiss LMS510 software (EMBL) in the format of 864×611 pixels, i.e., 326.3×291.5 μm. The laser scan was unidirectional and perpendicular to the EF direction in order to get rid of the temporal delay during image acquisition.

Image Analysis. The confocal images were processed using ImageJ software (National Institutes of Health). The fluorescence signal of the labeled siRNA in the cytoplasm was analyzed as follows: the first image (before EP) was subtracted from each image of the scan series. This process allowed the elimination of siRNA outside the cells and thus discriminated the labeled siRNA penetrating into the cells. A light profile oriented parallel to the EF direction was plotted across the cell in order to determine the orientation of the siRNA entrance. Then, the percentages of labeled cells on the cathode, anode, both, or no sides were calculated. A region of interest (ROI) was created limited by the internal periphery of each cell. The MFI of the same ROI was quantified for each image in the scan series.

Statistical Analysis. For the flow cytometry studies, three to five independent experiments were performed. For the microscopy studies and for each condition, more than 30 individual cells were analyzed (N represents the number of individual analyzed cells). Differences in percentages or relative fluorescence levels between the different conditions were statistically compared by using unpaired two-sided Student t-tests in Microsoft Excel software (version 2003). *** $P \leq 0.01$. The error bars represent the standard deviation of three independent measurements.

ACKNOWLEDGMENTS. This work was supported by grants from the Région Midi Pyrénées, the ITAV (Institut des Technologies Avancées en sciences du Vivant), the ANR (Agence Nationale de la Recherche) [Biodendridots (PCV06_136459) and Cemirbio (ANR-06-BLAN-0260-03) programs] and the European program (FP7 201102 OncomiR). We thank TRI (Toulouse Réseau Imagerie) Core facilities at the IPBS and Prof. Bettina Couderc for the generation of the B16F10-EGFP cells. Proof Reading Services corrected the manuscript.

1. Fire A, et al. (1998) Potent and specific genetic interference by double-stranded RNA in *Caenorhabditis elegans*. *Nature* 391:806–811.
2. Davis ME, et al. (2010) Evidence of RNAi in humans from systemically administered siRNA via targeted nanoparticles. *Nature* 464:1067–1070.
3. DeVincenzo J, et al. (2008) Evaluation of the safety, tolerability and pharmacokinetics of ALN-RSV01, a novel RNAi antiviral therapeutic directed against respiratory syncytial virus (RSV). *Antiviral Res* 77:225–231.
4. De Fougerolles A, Vornlocher HP, Maraganore J, Lieberman J (2007) Interfering with disease: a progress report on siRNA-based therapeutics. *Nat Rev Drug Discov* 6:443–453.
5. Behlke MA (2006) Progress towards in vivo use of siRNAs. *Mol Ther* 13:644–670.
6. Zhou J, Rossi JJ (2010) Aptamer-targeted cell-specific RNA interference. *Silence* 1:4–14.
7. Ledford H (2010) Drug giants turn their backs on RNA interference. *Nature* 468:487.
8. Liu J, et al. (2004) Argonaute2 is the catalytic engine of mammalian RNAi. *Science* 305:1437–1441.
9. Elbashir SM, et al. (2001) Duplexes of 21-nucleotide RNAs mediate RNA interference in cultured mammalian cells. *Nature* 411:494–498.
10. Mir LM (2009) Nucleic acids electrotransfer-based gene therapy (electrogenetherapy): past, current, and future. *Mol Biotechnol* 43:167–176.
11. Cemazar M, Sersa G (2007) Electrotransfer of therapeutic molecules into tissues. *Curr Opin Mol Ther* 9:554–562.
12. Berezhna SY, Supekova L, Supek F, Schultz PG, Deniz AA (2006) siRNA in human cells selectively localizes to target RNA sites. *Proc Natl Acad Sci USA* 103:7682–7687.
13. Golzio M, Teissie J, Rols MP (2002) Direct visualization at the single-cell level of electrically mediated gene delivery. *Proc Natl Acad Sci USA* 99:1292–1297.
14. Golzio M, et al. (2007) In vivo gene silencing in solid tumors by targeted electrically mediated siRNA delivery. *Gene Ther* 14:752–759.
15. Kishida T, et al. (2004) Sequence-specific gene silencing in murine muscle induced by electroporation-mediated transfer of short interfering RNA. *J Gene Med* 6:105–110.
16. Heller LC, Ugen K, Heller R (2005) Electroporation for targeted gene transfer. *Expert Opin Drug Del* 2:255–268.
17. Wells DJ (2004) Gene therapy progress and prospects: electroporation and other physical methods. *Gene Ther* 11:1363–1369.
18. Akaneya Y, Jiang B, Tsumoto T (2005) RNAi-induced gene silencing by local electroporation in targeting brain region. *J Neurophysiol* 93:594–602.
19. Takabatake Y, et al. (2005) Exploring RNA interference as a therapeutic strategy for renal disease. *Gene Ther* 12:965–973.
20. Matsuda T, Cepko CL (2004) Electroporation and RNA interference in the rodent retina in vivo and in vitro. *Proc Natl Acad Sci USA* 101:16–22.
21. Paganin-Gioanni A, Bellard E, Couderc B, Teissie J, Golzio M (2008) Tracking in vitro and in vivo siRNA electrotransfer in tumor cells. *Journal of RNAi and Gene Silencing* 4:281–288.
22. Jackson AL, Linsley PS (2010) Recognizing and avoiding siRNA off-target effects for target identification and therapeutic application. *Nat Rev Drug Discov* 9:57–67.
23. Low L, et al. (2009) DNA vaccination with electroporation induces increased antibody responses in patients with prostate cancer. . *Human Gene therapy* 20:1269–1278.
24. Daud AI, et al. (2008) Phase I trial of interleukin-12 plasmid electroporation in patients with metastatic melanoma. *J Clin Oncol* 26:5896–5903.
25. Gabriel B, Teissie J (1995) Control by electrical parameters of short- and long-term cell death resulting from electropermeabilization of Chinese hamster ovary cells. *Biochim Biophys Acta* 1266:171–178.
26. Gabriel B, Teissie J (1999) Time courses of mammalian cell electropermeabilization observed by millisecond imaging of membrane property changes during the pulse. *Biophys J* 76:2158–2165.
27. Tekle E, Astumian RD, Chock PB (1990) Electro-permeabilization of cell membranes: effect of the resting membrane potential. *Biochem Biophys Res Commun* 172:282–287.
28. Corish P, Tyler-Smith C (1999) Attenuation of green fluorescent protein half-life in mammalian cells. *Protein Eng* 12:1035–1040.
29. Baker M (2010) RNA interference: homing in on delivery. *Nature* 464:1225–1228.
30. Corey DR (2007) Chemical modification: the key to clinical application of RNA interference? *J Clin Invest* 117:3615–3622.
31. Soutschek J, et al. (2004) Therapeutic silencing of an endogenous gene by systemic administration of modified siRNAs. *Nature* 432:173–178.
32. Paroo Z, Corey DR (2004) Challenges for RNAi in vivo. *Trends Biotechnol* 22:390–394.
33. Pucihar G, Kotnik T, Miklavcic D, Teissie J (2008) Kinetics of transmembrane transport of small molecules into electropermeabilized cells. *Biophys J* 95:2837–2848.
34. Maucksch C, et al. (2009) Transgene expression of transfected supercoiled plasmid DNA concatemers in mammalian cells. *J Gene Med* 11:444–453.
35. Wanunu M, et al. (2010) Rapid electronic detection of probe-specific microRNAs using thin nanopore sensors. *Nat Nanotechnol* 5:807–814.
36. Branton D, et al. (2008) The potential and challenges of nanopore sequencing. *Nat Biotechnol* 26:1146–1153.
37. Kasianowicz JJ, Brandin E, Branton D, Deamer DW (1996) Characterization of individual polynucleotide molecules using a membrane channel. *Proc Natl Acad Sci USA* 93:13770–13773.
38. Heng JB, et al. (2006) The electromechanics of DNA in a synthetic nanopore. *Biophys J* 90:1098–1106.
39. Hibino M, Shigemori M, Itoh H, Nagayama K, Kinosita K, Jr (1991) Membrane conductance of an electroporated cell analyzed by submicrosecond imaging of transmembrane potential. *Biophys J* 59:209–220.
40. Teissie J, Rols MP (1993) An experimental evaluation of the critical potential difference inducing cell membrane electropermeabilization. *Biophys J* 65:409–413.
41. Hajeri PB, Singh SK (2009) siRNAs: their potential as therapeutic agents–Part I. Designing of siRNAs. *Drug Discov Today* 14:851–858.
42. Kariko K, Bhuyan P, Capodici J, Weissman D (2004) Small interfering RNAs mediate sequence-independent gene suppression and induce immune activation by signaling through toll-like receptor 3. *J Immunol* 172:6545–6549.
43. Ferrari M (2010) Frontiers in cancer nanomedicine: directing mass transport through biological barriers. *Trends Biotechnol* 28:181–188.
44. Caplen NJ, Parrish S, Imani F, Fire A, Morgan RA (2001) Specific inhibition of gene expression by small double-stranded RNAs in invertebrate and vertebrate systems. *Proc Natl Acad Sci USA* 98:9742–9747.
45. Mazeres S, et al. (2009) Non invasive contact electrodes for in vivo localized cutaneous electropulsation and associated drug and nucleic acid delivery. *J Control Release* 134:125–131.
46. Rols MP, Teissie J (1998) Electropermeabilization of mammalian cells to macromolecules: control by pulse duration. *Biophys J* 75:1415–1423.